Available online at www.sciencedirect.com
SCIENCE DIRECT®
ELSEVIER
Earth and Planetary Science Letters 213 (2003) 31–42
EPSL
www.elsevier.com/locate/epsl

Sm–Nd dating of spatially controlled domains of garnet single crystals: a new method of high-temperature thermochronology

Mihai N. Ducea *, Jibamitra Ganguly, Erin J. Rosenberg [1], P. Jonathan Patchett, Weiji Cheng, Clark Isachsen

University of Arizona, Department of Geosciences, Tucson, AZ 85721, USA

Received 3 April 2003; accepted 23 May 2003

Abstract

Ganguly and Tirone [Meteorit. Planet. Sci. 36 (2001) 167–175] recently presented a method of determining the cooling rates of rocks from the difference between the core and bulk ages of a crystal, as determined by a single decay system. Here we present the first application of the method using the core and bulk ages of garnet single crystals, according to the Sm–Nd decay system, in two rock samples with contrasting cooling rates, which can be constrained independently. The samples belong to the metamorphic core complex, Valhalla, British Columbia, and the mid-crustal magmatic arc exposure of the Salinian terrane, California. We have micro-sampled the garnet crystals over specific radial dimensions, and measured the Nd isotopes of these small sample masses, as NdO^+ via solid source mass spectrometry, to determine the Sm–Nd age difference between the core and bulk crystals. Using a peak metamorphic *P–T* condition of 8 ± 1 kbar, 820 ± 30°C [Spear and Parrish, J. Petrol. 37 (1996) 733–765], the core (67.3 ± 2.3 Ma) and bulk (60.9 ± 2.1 Ma) ages of the British Columbian garnet sample yield a cooling rate of 2–13°C/Myr, which is in very good agreement with the cooling rates that we have derived by modeling the retrograde Fe–Mg zoning in the same garnet, and assuming the same peak metamorphic *P–T* condition. Considering earlier cooling rate data derived from closure temperature vs. age relation of multiple geochronological systems [Spear and Parrish, J. Petrol. 37 (1996) 733–765], a cooling rate of ~15–20°C/Myr seems most reasonable for the Valhalla complex. Diffusion kinetic analysis shows that the Sm–Nd core age of the selected garnet crystal could not have been disturbed during cooling. Consequently, the core age of the garnet crystal, 67.3 ± 2.3 Ma, corresponds to the peak metamorphic age of the Valhalla complex. The Salinian sample, on the other hand, yields indistinguishable core (78.2 ± 2.7 Ma) and bulk (77.9 ± 2.9 Ma) ages, as expected from its fast cooling history, which can be constrained by the results of earlier studies. The Sm–Nd decay system in garnet has relatively high closure temperature (usually >650°C); therefore, the technique developed in this paper fills an important gap in thermochronology, since the commonly used thermochronometers are applicable only at lower temperatures. Simultaneous modeling of the retrograde Fe–Mg zoning in garnet, spatially resolved Sm–Nd ages of garnet single crystals, and resetting of the bulk garnet Sm–Nd age

* Corresponding author.
E-mail address: ducea@geo.arizona.edu (M.N. Ducea).

[1] Present address: Dartmouth College, Department of Earth Sciences, Hanover, NH 03755, USA.

0012-821X/03/$ – see front matter
doi:10.1016/S0012-821X(03)00298-X

from the peak metamorphic age [Ganguly et al., Science 281 (1998) 805–807], along with additional geochronological data, would lead to robust constraints on cooling rates of rocks.

Keywords: Nd isotopes; garnet; single crystal; thermochronology

1. Introduction

Significant areas of the continents expose metamorphic rocks that at some stage were buried to depths equal to or greater than the normal thickness of the continental crust (30–40 km). The processes by which high-pressure rocks reach great depths are generally accepted to be shortening and thickening of the crust, and lithospheric subduction (e.g. [4]). How rocks subsequently return to the surface is an intriguing question that has generated considerable interest among geologists [5]. Understanding the exhumation mechanisms of orogenic roots requires quantification of the pressure–temperature–time (*P–T–t*) paths of these rocks. Commonly the *P–T* paths are deciphered without age constraints. The cooling and the related exhumation rates are commonly derived from plots of selected mineral ages versus assumed or inferred closure temperatures of the specific geochronologic systems. Exhumation rates determined this way vary by approximately two orders of magnitude (e.g. [6], for a review). Some of this variability is related to uncertainties in closure temperatures. Other additional problems are whether a mineral age dated by a particular system corresponds to peak metamorphic age, cooling age, or, in some cases, is an average of various ages in rocks with complex, polyphase histories [7,8].

Closed-form analytical expressions of closure temperature (T_c) and T_c-profile in a mineral that is surrounded by a homogeneous infinite matrix during cooling were derived by Dodson [9,10]. However, although it is commonly overlooked, Dodson's T_c formulations are applicable only to cases where the composition of the mineral, even at the core, is significantly removed from what it was at the onset of cooling. Consequently, this formulation is not applicable to the cases of slowly diffusing species or when the diffusion distance is small compared to the grain size. Ganguly and Tirone [11] extended Dodson's formulation to include the cases of the slowly diffusing species, such as Sm and Nd in garnet, and developed [1,11] mathematical formulations and algorithms that permit retrieval of cooling rate from the cooling age profile, or from the difference between the core and bulk ages of a single crystal, and its initial temperature (T_0), provided that the diffusion kinetic properties of the decay system are known. The diffusion kinetics of Sm and Nd in almandine garnet have recently been determined by Ganguly et al. [3]. These data, along with the formulation in [1], permit quantitative use of the spatial variation of Sm–Nd age within a garnet crystal as a high-temperature thermochronometer.

A significant practical problem in the application of the Ganguly–Tirone formulation [1] is the difficulty in obtaining single garnet age profiles, or the average (Sm–Nd) age of the garnet core on a sufficiently small spatial scale ($\leq 50\%$ of the grain size) such that it is distinctly different from the bulk or rim (Sm–Nd) age. In this study we overcome this difficulty by: (a) using a milling device that can sample to μ-scale resolution, and (b) analyzing small Nd quantities as NdO^+ via thermal ionization mass spectrometry.

Spatially resolved Sm–Nd dating of garnet single crystals has been conducted previously (e.g. [12–15]). However, these studies utilized large crystals that preserved prograde growth zoning with the objective of determining the rates of crystal growth or unraveling the timing of poly-metamorphic events. This is the first study aimed at recovering high-temperature cooling rate from dating core and rim of single garnet crystals.

2. Theoretical background

The theoretical foundation of Sm–Nd thermo-

chronology lies in the works of Dodson [9,10] and its recent extensions by Ganguly and Tirone [1,11]. Thus, only a brief exposition of the concepts is provided below. When a mineral with slow diffusion properties, such as garnet, cools from an initial temperature at which it has attained a homogeneous composition, it develops a retrograde zoning profile since the equilibration of the core with the surrounding matrix lags behind that of the interface during cooling. In this case, the zoning profile of an element freezes over a range of temperatures (highest in the core and lowest at the rim), leading to a closure temperature profile (T_c-profile) instead of a discrete T_c. Consequently, the mineral also develops an age profile (or t-profile) since the decay system used in dating the mineral freezes within the latter at different temperatures. Thus, both the conventional closure temperature and age of a mineral with slow diffusion properties such as garnet represent weighted averages over the entire grain.

Ganguly and Tirone [11] derived the mathematical expressions (and developed the related computer programs) for the calculations of the T_c- and t-profiles, and the corresponding weighted mean quantities over specific spatial domains of a crystal. As in Dodson [9,10], the cooling was assumed to follow an asymptotic relation:

$$\frac{1}{T} = \frac{1}{T_0} + \eta t \tag{1}$$

where T_0 is the initial temperature and η is the cooling time constant (with dimension of K^{-1} t^{-1}). Since t-profile is a difficult quantity to measure with the present techniques, Ganguly and Tirone [1] reformulated the spatial variation of age in terms of the difference between the weighted average of the age of a central segment of defined dimension and that for the bulk crystal. We would refer to this age difference as Δt(core–bulk). They also presented graphical charts showing the relationship among Δt(core–bulk), η, and a dimensionless variable, M, which is defined as follows:

$$M = \frac{RD(T_0)}{E\eta a^2} \tag{2}$$

where R is the gas constant, $D(T_0)$ is the diffusion coefficient at the peak temperature (T_0), E is the activation energy of diffusion, and a is a characteristic grain dimension (radius of a sphere or cylinder and half-thickness of a plane sheet). Analytically, Δt(core–bulk) can be calculated from the relation [11]:

$$\Delta t(\text{core} - \text{bulk}) = -\frac{R}{E\eta}[\Delta G + \Delta g] \tag{3}$$

where the Δ on the right hand side stands for the difference of the specified quantity between its weighted average values for a central domain and for the bulk crystal. Here G is a function only of the normalized position (x) in the crystal [10], whereas g is a function of both x and M [11]. Because of the nature of Eq. 3, the cooling time constant has to be calculated by successive approximations from a measured Δt(core–bulk) value. That is, one must calculate Δt(core–bulk) from a guessed value of η and the corresponding value of g via M, and see if it matches the measured value.

In developing the above concepts, it was assumed, following Dodson [9,10], that the mineral of interest is surrounded by a homogeneous and effectively infinite matrix. This condition may not always be satisfied. However, when it is satisfied, it should lead to a larger Δt(core–bulk) than otherwise. Consequently, the cooling rate deduced from the measured Δt(core–bulk) should represent an upper bound to the true cooling rate. The practical strategy to ensure that the boundary condition is closely satisfied would be to select garnet crystals with the largest compositional difference between core and rim from rocks in which the modal abundance of garnet is small ($< 10\%$). The boundary condition may be satisfied, as recently demonstrated experimentally [16], even when the relatively abundant matrix minerals have slow volume diffusion property, since the material exchanged with the target mineral is rapidly distributed over a large volume of the grain boundary domains through rapid grain boundary diffusion.

3. Analytical techniques

3.1. Sample preparation

Thin sections were cut from whole-rock samples and utilized for petrographic and electron microprobe analyses. The accompanying thick section slab is then used to micro-sample garnet and obtain whole-rock separates. The electron microprobe analyses of major cation distribution within garnet crystals and surrounding medium resolve the nature of compositional zoning in garnet, and help constrain the peak metamorphic *P–T* conditions. In this study, we are interested in garnets exhibiting only retrograde zoning profiles. In order to ensure that the true core of a garnet is being sampled, a three-dimensional (3-D) view of the thick section is needed. Such 3-D images can be obtained by computer-aided X-ray tomography [17]. However, in the present exploratory study, we avoided this time-consuming and expensive approach, but instead carefully selected garnet grains with relatively larger (apparent) diameters on the cut surface of the rock samples, and assumed that these grains were cut close to their respective central sections.

3.2. Micro-sampling

Thick sections were micro-sampled using a Micromill instrument (designed by NewWave-Merchantek), which can extract materials over as small as a few μm in diameter. Combination of sub-μm stage resolution and positional accuracy, real-time video observation and a custom-designed software system allows for sampling of complex crystalline materials such as garnets or other silicates. One of the most important features is the computer routine for interpolation of sampling paths and on-screen display of digitized sampling paths. This allows the sampling to be conducted automatically on pre-determined paths and with desired depths, no matter how complicated. Transmitted and/or reflected light microscopy can be used for sampling. In this study, we used diamond drill bits from Brasseler Instruments in order to be able to efficiently drill through garnet grains. Overall, the sample recovery is about 85–90%. Inclusions visible optically are easily avoided along the sampling paths.

3.3. Column chemistry and TIMS analyses

The mineral separates are put in Teflon beakers and dissolved in mixtures of hot concentrated $HF–HNO_3$. To ensure complete dissolution of fluorides, samples were dried-down and immediately re-dissolved in 6 N HCl-concentrated H_3BO_3 mixed in 4:1 proportions. The dissolved samples are spiked with a mixed Sm–Nd spike [18] after dissolution. Bulk rare earth elements were separated in 0.1 ml volume Eichrom TruSpec cation-exchange columns eluted with 0.05–2 N HNO_3. Separation of Sm and Nd is achieved in anion columns containing LN Spec resin, using 0.1–2.5 N HCl [19,20]. The second-stage column step is performed twice in order to reduce the chance of Pr interference.

Sm and Nd were loaded in HCl onto single Re filaments. Mass spectrometric analyses for Sm were carried out on a 54 VG Sector multi-collector instrument following the procedures in [19]. Neodymium was measured as an oxide [18] on a 354 VG Sector instrument fitted with a purified oxygen tube and a bleed valve delivering oxygen into the source. Pr and Ce interference was monitored, and no interference from these elements was observed.

On- and off-line manipulation programs were used for isotope dilution calculations. The runs consisted of 105 isotopic ratios for Nd and 60 ratios for Sm. The mean results of five analyses of the standard nSmβ performed during the course of this study are: $^{148}Sm/^{147}Sm = 0.74880 \pm 21$ and $^{148}Sm/^{152}Sm = 0.42110 \pm 6$. Nine measurements of the LaJolla Nd standard measured as oxide were performed during the course of this study which coincided with the installation of the bleed valve attachment, and yielded results within the accepted range of LaJolla $^{143}Nd/^{144}Nd$ (mean $^{143}Nd/^{144}Nd = 0.5118490 \pm 23$). Fig. 1 is a plot of LaJolla $^{143}Nd/^{144}Nd$ values measured as oxide, obtained during the course of this study. The Nd isotopic ratios were normalized to $^{146}Nd/^{144}Nd = 0.7219$. Standard loads as small as 5 ng Nd were successfully analyzed. Fractions (core

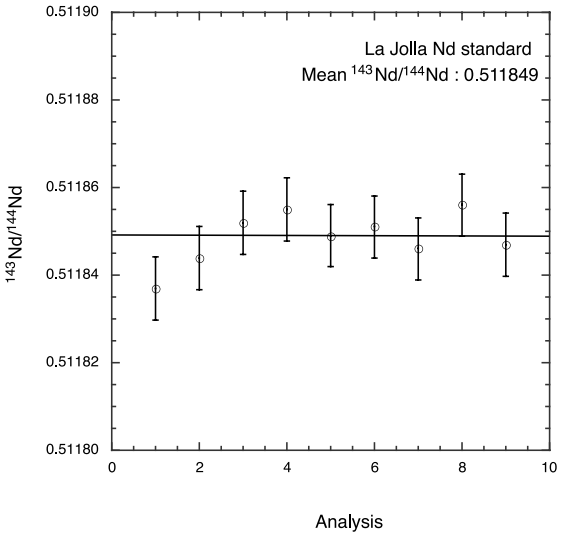

Fig. 1. Results of runs of $^{143}Nd/^{144}Nd$ as NdO^+ for the standard LaJolla, analyzed during the course of this study.

and rim) of garnet BC207 [19] were analyzed as unknowns and yielded results consistent with previous, multigrain analyses. A few measurements of Nd metal were also performed in this study in order to check the precision of the NdO^+ analyses.

4. Samples and cooling rates

In order to determine cooling rates from the core and bulk ages of a garnet single crystal, we selected two samples, one from the Valhalla complex, British Columbia, and the other from the Salinian terrane, coastal California. The cooling rates of these samples are very different and can be well constrained by independent methods. The geological background of the samples and their cooling rates, as constrained independently and from the difference between the core and bulk Sm–Nd ages, are discussed below. The isotopic results are shown in Table 1.

Table 1
Neodymium isotopic data

Sample	Mass Nd[a] (ng)	Type analysis[b]	Sm (ppm)	Nd (ppm)	$^{147}Sm/^{144}Nd$[c]	$^{143}Nd/^{144}Nd$[d]	Age[e] (Ma)
Paragneiss V7C-Grf, Valhalla complex, British Columbia [2]							
Biotite matrix 1	2460.5	Elem	5.79	34.74	0.101	0.5118853 ± 8	
Biotite matrix 2[f]	88.9	Ox	5.66	33.91	0.101	0.5118849 ± 9	
Garnet core ($r/a = 0.4$[g])	75.0	Ox	2.69	3.46	0.471	0.5120477 ± 10	67.3 ± 2.3
Garnet rim	250.3	Ox	4.18	7.21	0.352	0.5119831 ± 12	59.8 ± 2.0
Garnet rim replicate	475.5	Ox	4.05	7.05	0.348	0.5119836 ± 11	61.1 ± 2.2
Bulk garnet[h]		Calc			0.357	0.5119870 ± 9	60.9 ± 2.1
Garnet tonalite 730-4, Cone Peak, central California [32]							
Biotite matrix	105.5	Ox	5.00	19.81	0.152	0.5126390 ± 8	
Garnet core ($r/a = 0.5$)	62.3	Ox	6.87	8.25	0.504	0.5128061 ± 11	78.2 ± 2.7
Garnet rim	85.5	Ox	6.22	7.55	0.499	0.5128152 ± 12	77.6 ± 3.0
Bulk garnet[h]		Calc			0.500	0.5128140 ± 11	77.9 ± 2.9
Garnet multigrain[i]	1980.2	Elem	6.48	7.84	0.500	0.5128120 ± 11	76.5 ± 1.5

[a] (Mass of dissolved sample) × (Nd concentration). About half of this amount was loaded onto the mass spectrometer for analysis.
[b] 'Elem', Nd analyzed as metal, as described in [18,19]; 'Ox', Nd isotopes measured as oxides (see Section 3); 'Calc', calculated by material balance using core and rim data.
[c] Parent:daughter ratios are precise to about 0.25%.
[d] Standard error given in 2σ.
[e] Age errors (2σ) were calculated using Ludwig [35] and are analytical only.
[f] Represents the 'whole-rock' medium surrounding the garnet grain.
[g] r is radius of the core sample, a is radius of garnet grain.
[h] Calculated from material balance.
[i] From Kidder et al. [32].

4.1. Valhalla complex, British Columbia

4.1.1. Geological background and selection of garnet crystal

The Valhalla complex is one of the fault-bounded metamorphic core complexes that form the Shuswap complex of southern British Columbia. It had experienced upper amphibolite to lower granulite facies metamorphism in the late Cretaceous period [2,21]. Spear and Parrish [2] constrained the cooling rates of these samples to be 24 ± 6°C/Myr, using T_c vs. age relations of multiple geochronologic systems, from a peak P–T condition of 8 ± 1 kbar, 820 ± 30°C, which they calculated from conventional thermo-barometric methods. A sample from the collection of these workers (sample No. V7C) was used in this work. The rock consists of garnet, biotite, sillimanite, K-feldspar, plagioclase, quartz, ilmenite and rutile. Garnets range from 6 to 12 mm in apparent diameter in a polished surface of this sample. We chose the largest garnet crystal for analysis and sampled the entire crystal, avoiding monazite and biotite inclusions. A Mg X-ray map of the garnet crystal and the surrounding matrix is shown in Fig. 2A. Because of its size, it was assumed that the chosen garnet crystal was cut along its central section or very close to it.

We measured the compositional zoning of garnet adjacent to matrix biotite along several traverses, which are normal to the trace of the interface on the polished section. These traverses are shown as straight lines within the garnet crystal in Fig. 2A. Compositional profiles along all traverses are found to be similar, showing homogeneous core, retrograde Fe–Mg zoning near the rim, and essentially flat profiles for Ca and Mn from core to rim. Fig. 3A shows the compositional profiles of Fe, Mg, Ca and Mn along the traverse labeled (X) in Fig. 2A.

Spear and Parrish [2] and Spear (personal communication, 2003) have discussed evidences of resorption of garnet as well as late overgrowth of garnet on garnet in the Valhalla samples. However, the Mg X-ray map (Fig. 2A) and the compositional profiles (Fig. 3A) of the garnet crystal *selected* for this study do not show any evidence of late overgrowth. Instead, the compositional zoning is what one would expect from retrograde exchange between garnet and matrix biotite. If there were any late overgrowth of garnet on a pre-existing garnet core, then one would not expect to see a flat Ca profile, unless the atomic

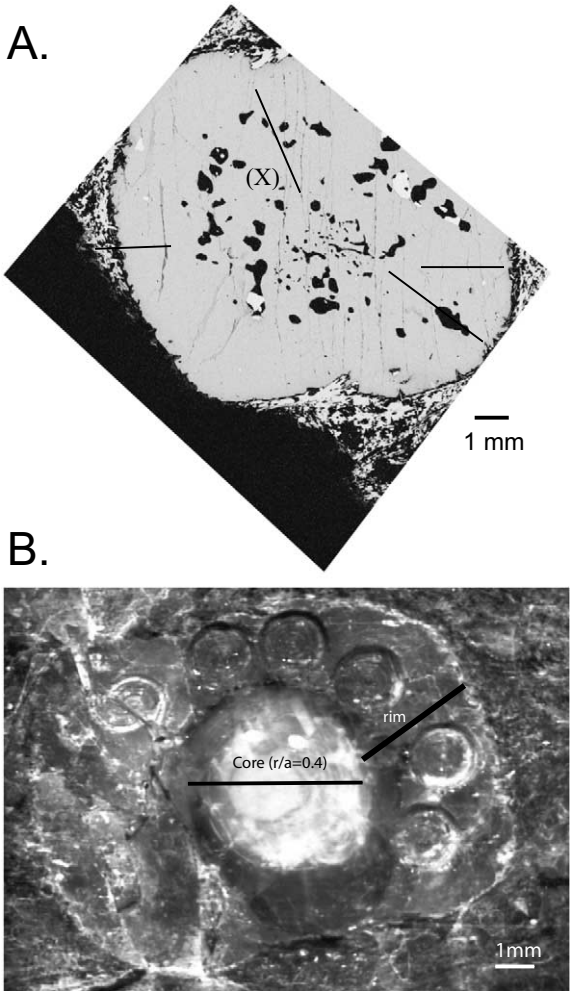

Fig. 2. (A) Mg X-ray map of the selected garnet crystal and the surrounding matrix in the sample V7C [2] from the Valhalla complex, British Columbia. The solid lines show traverses along which compositional zoning of garnet was measured. The compositional zoning along the traverse (X) is shown in Fig. 3. Few bright biotite inclusions, but not the abundant quartz inclusions seen in the center and middle, have been avoided during micro-sampling. (B) Photograph of the same garnet after the core region has been milled out, and during the process of rim extraction. The pits drilled in this garnet were 130 μm deep.

fraction of Ca in the overgrowth fortuitously happened to be exactly the same as that of the core, which is extremely unlikely. Additionally, we would expect to see inflections on the Mg and Fe profiles of garnet owing to the initial difference in the atomic fractions of these components in the core and overgrowth segments. No such inflection is, however, visible in the measured concentration profiles. We therefore conclude that the difference between the core and rim Sm–Nd ages of the selected garnet crystal is essentially due to the diffusive resetting of the age near the rim during cooling.

4.1.2. Cooling rate

Since Fe and Mg are the only two components that seem to have been significantly affected by diffusion, we have treated the compositional zoning data in terms of a binary diffusion problem, and normalized the measured data accordingly. The Mg/(Mg+Fe) data along the traverse (X) are shown in Fig. 3B. These data were modeled to constrain the high-temperature cooling rate of the Valhalla complex. The details of the method, which is based on a modification of Lasaga's theory [22], are given in Ganguly et al. [23]. In this work, we have also incorporated the effect of a moving boundary that could take place due to the possible resorption of garnet during cooling, and treated the location of the boundary as an additional floating variable.

A finite-difference program implementing the diffusion equation was interfaced with a non-linear optimization program to find the best combination of values (within specified ranges) of the different governing parameters such that the calculated profile represents the statistical best fit to the observed data, within the framework of the adopted model. These parameters are: (a) the initial composition of garnet; (b) the value of the ratio $\Delta H^0/Q$, where ΔH^0 is the enthalpy change of the exchange reaction between garnet and biotite and Q is the activation energy of Fe–Mg inter-diffusion in garnet; (c) the position of the interface; and (d) the dimensionless parameter M (Eq. 2). All these parameters were treated as floating variables. The initial composition of garnet was assumed to be homogeneous, while the boundary concentration was assumed to change according to equilibrium Fe–Mg exchange during cooling (Eq. 1) with a biotite matrix, which remained homogeneous because of relatively much faster diffusivity of the components, as evidenced by their uniform composition. The mass abundance of the biotite matrix adjacent to garnet was assumed to be sufficiently large to maintain an effectively fixed composition (the potential ef-

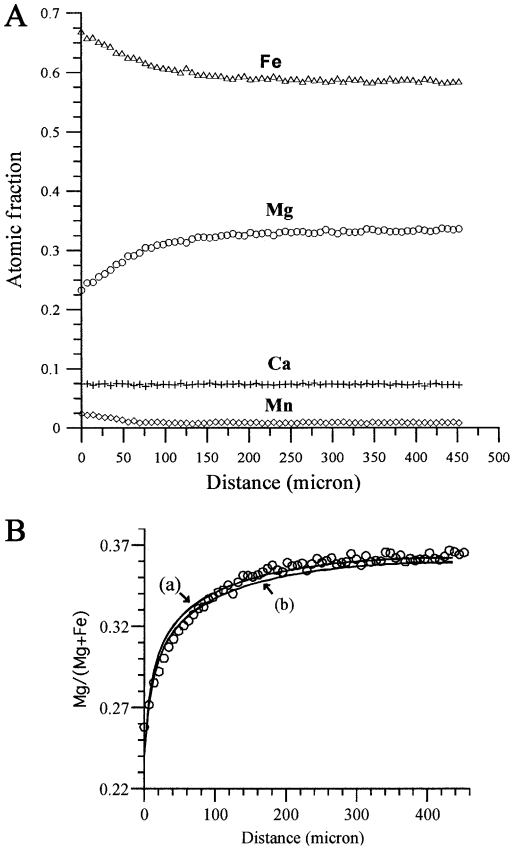

Fig. 3. (A) Major element compositional profiles of the garnet sample from the Valhalla complex, British Columbia, along the traverse (X) shown in Fig. 2A. (B) Mg/(Mg+Fe) profile calculated from the data, which are illustrated in Fig. 2A. The measured electron microprobe data are shown by open circles. The curve (a) is an optimized fit to the data according to the numerical solution of the diffusion equation incorporating the effect of changing interface equilibrium during cooling, and assuming a non-linear cooling model (Eq. 1). The curve (b) is calculated by forcing the profile to better fit the data near the interface.

fect of change of biotite composition is discussed below).

The above procedure resulted in a model of stationary interface and fixed core composition as the best model, and yielded the profile (a) in Fig. 3B, as the best fit to the data for the development of compositional zoning in garnet, satisfying the above initial and boundary conditions. The curve (b) in Fig. 3B was calculated by forward modeling without using the optimization program, to better fit the data near the grain boundary. The interface was treated as stationary, and the ratio of $\Delta H^0/Q$ was set equal to 0.058. The latter was obtained from the optimization analysis that led to the curve (a), and is compatible with the available experimental data [24,25]. In the calculation of both profiles (a) and (b), the Fe–Mg inter-diffusion coefficient, D(Fe–Mg), was assumed to be insensitive to the compositional changes within the diffusion zone. It was calculated at the median composition of the diffusion zone from the self-diffusion data of Fe and Mg in garnet [25], according to the relationship between the self- and inter-diffusion coefficients of equally charged ionic species in an ideal binary solid solution (e.g. [25]). The assumption of ideality of mixing of Fe and Mg in garnet is justified according to the experimental studies on the thermodynamic mixing behavior of these cations in garnet [26].

Using the D(Fe–Mg) value at $T_0 = 820$°C, we obtain $\eta = 4.8 \times 10^{-6}$ K^{-1} Myr^{-1} for the curve (a) and $\eta = 3.6 \times 10^{-6}$ K^{-1} Myr^{-1} for the curve (b) from the respective M values that were retrieved from modeling of the retrograde zoning in garnet, as discussed above. These η values yield initial cooling rates (according to $\mathrm{d}T/\mathrm{d}t = -\eta T^2$, see Eq. 1) of 4–6°C/Myr for the Valhalla sample. The uncertainties of the inferred peak P–T condition (± 1 kbar, ± 30°C) expand the permissible range of cooling rate to 2–13°C/Myr.

Spear and Parrish [2] suggested that retrograde compositional zoning in the Valhalla samples developed, at least in some cases, as a result of diffusion during net transfer reaction, which could lead to change of both biotite and garnet rim composition in the same direction. We discuss here the potential error in the above cooling rate calculation if the biotite composition had indeed changed in the same direction as garnet. In order to have the appropriate value of the Fe–Mg distribution coefficient at a given temperature, the change of garnet composition would be more when the biotite gains Fe (and looses Mg) during cooling relative to the case in which its composition had remained fixed. Consequently, the cooling rate will be underestimated if the compositional profile that was produced by maintaining interface equilibrium with a biotite matrix of changing composition was modeled by assuming that the biotite composition had remained fixed. However, we have not seen any evidence of retrograde net transfer reaction at the garnet rim and adjacent matrix at the termination of the traverse (X), and also, based on our experience (e.g. [16]), we think that it is unlikely that diffusion zoning produced by one process can be fitted adequately by a model based on a significantly different process.

Using the Sm–Nd data for the core–whole rock and rim–whole rock, we obtained Sm–Nd ages of 67.3 ± 2.3 Ma for the core and 59.8 ± 2 Ma for the rim of the chosen garnet crystal from the Valhalla complex (Fig. 4). The ratio of the radial dimensions of the core and the bulk crystal is 0.4. The calculated bulk age is 60.9 ± 2.1 Ma. Using Eqs. 2 and 3, the relevant data for the spatially averaged G and g parameters [1], the tracer diffusion data of Nd in almandine garnet [3], and $T_o = 820$°C, we obtain $\eta = (5.1\text{–}8.3) \times 10^{-6}$ K^{-1} Myr^{-1}, and hence an initial cooling rate of 6–10°C/Myr. Propagating the uncertainties of the initial condition expands the range of cooling rate to 4–13°C/Myr.

In the above calculations, we did not propagate the errors arising from those in the diffusion data. However, it is remarkable that the cooling rates obtained from two independent methods and two sets of diffusion data, one for the divalent cations [25] and the other for Nd [3], are in excellent agreement with one another. Comparing these results with the cooling rate of 24 ± 6°C/Myr that was deduced from the T_c vs. age relations of multiple geochronological systems [2], and bearing in mind that there are also additional uncertainties in the T_c values as these depend on cooling rate itself and grain size [3,9], it seems reasonable to

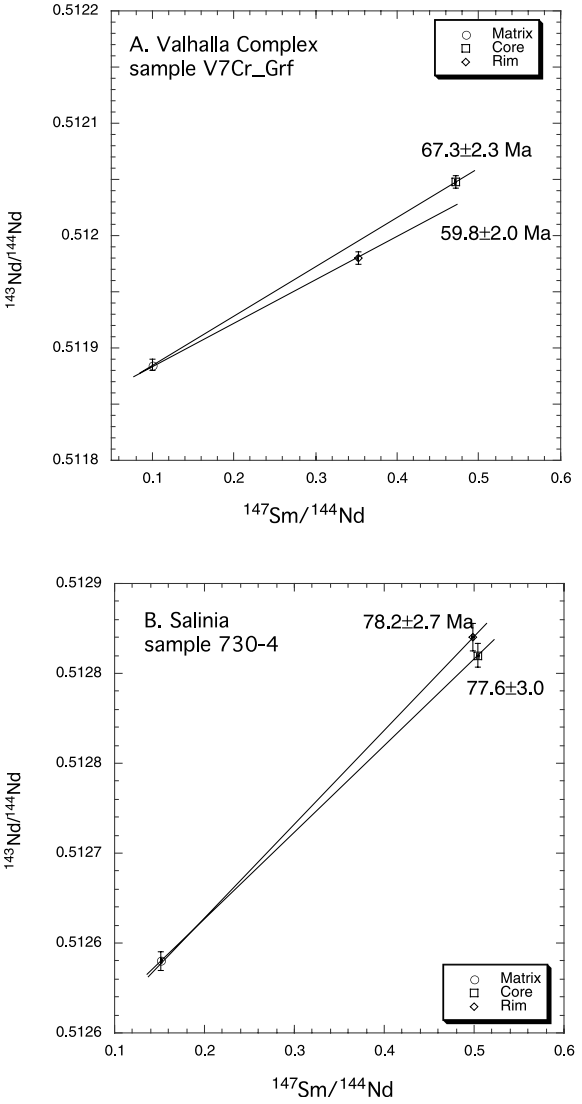

Fig. 4. Single crystal neodymium isochron diagrams for (A) the Valhalla complex paragneiss and (B) the Cone Peak garnet tonalite. Shown in the diagram are the ages of garnet cores and rims. The bulk garnet ages, as calculated by material balance, are not shown. Uncertainties are reported in Table 1.

suggest ~15–20°C/Myr as the most likely range of cooling rate of the Valhalla complex.

4.1.3. Peak metamorphic age

Using U–Pb zircon geochronology, Spear and Parrish [2] determined the peak metamorphic age of 75 ± 5 Ma. Recently, however, Spear (personal communication, 2003) suggested that this age does not necessarily indicate the peak metamorphic age of the complex. The modeling of retrograde compositional zoning incorporating optimization analysis, as discussed above, indicates that the Fe–Mg core composition of the selected garnet crystal was not affected by diffusion during cooling. Since the diffusivity of Nd is comparable to that of Mg [3], we suggest that the core Sm–Nd age of the garnet crystal of 67.3 ± 2.3 Ma, as determined in this study, represents the peak metamorphic age of the Valhalla complex. This conclusion also follows from the calculation of cooling rate that would be required to significantly affect Sm–Nd age of the core, and comparison with the cooling rate derived from geochronological constraints [2].

An upper limit of cooling rate that would be needed to significantly affect the core composition can be derived from the solution of the diffusion equation for a sphere with fixed surface composition that is different from the initial homogeneous composition. This would be an upper limit since, in reality, the boundary concentration would change continuously with temperature during cooling, thereby producing a smaller concentration gradient, and hence smaller diffusive flux, relative to the case in which the boundary concentration had changed instantaneously to the extreme value. Under isothermal condition, the minimum value of Dt/a^2, where a is the radius of the spherical grain, is 0.04 ([27], p. 92). Under non-isothermal condition, Dt can be replaced by $\int D(t)\mathrm{d}t$ ([27], p 104). If the inverse temperature varied linearly with time during cooling, as assumed in this study (Eq. 1), then we have, for $t \gg 0$ [28]:

$$\int_0^{t'} D(t)\mathrm{d}t = \frac{RD(T_0)}{Q\eta} \tag{4}$$

Using the diffusion data for Nd in almandine garnet [3], we then obtain $\eta = 5\times10^{-6}$ K^{-1} Myr^{-1}. This yields a cooling rate of ≤4°C/Myr at 600°C, which is too slow compared to that (24 ± 6°C/Myr) constrained by the geochronological data [2].

5. Garnet tonalite from Cone Peak, California

5.1. Geological background

The Coast Ridge Belt, central Coastal California, exposes upper amphibolite to granulite facies mid-crustal rocks of a Cretaceous magmatic arc, part of the Salinian terrane [29]. Salinia is a predominantly magmatic arc terrane that originated near the present-day Mojave region and was translated northwards along San Andreas and related faults [30]. The Coast Ridge Belt rocks represent the deepest exposure of the now dissected Salinian arc, and are overlain by Late Cretaceous–Cenozoic sedimentary rocks predominantly exposed on the northeastern and southern limits of the range [31]. The rock analyzed here (730-4) is part of the 80 Ma Cone Peak garnet tonalite [32]. Peak *P–T* conditions on this rock are 8 kbar, 750°C [32]. Multigrain garnet Sm–Nd geochronology indicates that garnet grew at $\sim$76.5 ± 1.5 Ma while these rocks were buried at $\sim$25–26 km [32]. Mid–late Maastrichtian ($\sim$70 Ma) sandstones rest unconformably immediately above the Cone Peak intrusion in this section [33]. The Cone Peak rocks had thus exhumed at a rate of $>$3 mm/yr [32], and cooled quickly below the closure temperatures of biotite K–Ar (75 Ma [30]) and apatite fission track (74 ± 5 Ma [34]) systems. Cooling from peak temperature conditions ($\sim$750°C) to below 200°C must have taken place within 2–4 Myr

5.2. Cooling rate from single crystal age data

We reanalyzed sample 730-4 for single crystal garnet chronology (Table 1) as an end-member rock that should yield no differences between core and bulk Sm–Nd ages, given the above constraints. The garnet crystal used in this study is surrounded by a biotite-rich selvage. Therefore, it was assumed that the biotite was in equilibrium with the garnet during its growth. The crystal of garnet is 0.8 cm in diameter and the diameter of the core sampled here represents half of this dimension. The Cone Peak garnet has very few plagioclase inclusions and is essentially devoid of high-Nd (monazite, zircon, apatite) inclusions, which resulted in an almost complete sampling of the selected garnet. The results are indistinguishable from the earlier multigrain analysis (76.5 ± 1.5 Ma) and are shown in Fig. 4. Within the error of our analysis there is no age difference between core (78.2 ± 2.7 Ma) and bulk (77.9 ± 2.9 Ma) ages in this case, although the Sm/Nd ratios of the core and rim of the garnet are slightly different. This result and previous data imply an initial cooling rate $>$100°C/Myr for this sample.

6. Discussion

We have successfully separated and analyzed Nd isotopes on core and rim fractions of single garnet crystals from high-grade metamorphic rocks, and used the difference between the core and bulk ages to determine the cooling rates of the samples, along with constraining the peak metamorphic age of the Valhalla complex. Since the Sm–Nd decay system in garnet has a relatively high closure temperature (usually $>$650°C; [10]), this technique can be applied to decipher the initial cooling and exhumation path of garnet-bearing metamorphic rocks, and would therefore fill an important gap in thermochronological studies. In addition, use of this technique in conjunction with the modeling of retrograde Fe–Mg zoning in garnet, which yields independent cooling rate over essentially the same temperature interval, as well as the cooling rate constrained by the extent of resetting of the bulk Sm–Nd age of a garnet crystal [3] and other geochronological constraints, would provide robust constraint on the cooling rate of rocks.

We tested the technique of the determination of cooling rate from the difference between the core and bulk Sm–Nd ages of a garnet crystal on two samples from regions that have been previously studied and where the cooling rates can be quantified independently. On both samples, the cooling rates obtained from the Sm–Nd age data of core and bulk of garnet single crystals were found to be in good agreement with those constrained independently. The technique has several advantages over conventional geochronology in that: (a) it provides cooling rate in addition to cooling

age without any appeal to closure temperature; (b) inclusion-free material can be selectively used for analyses; (c) it requires a small sample size; and (d) the Sm–Nd core age of garnet of appropriate size could yield the peak metamorphic age, as we have illustrated for the Valhalla sample.

Acknowledgements

This work was funded by Grant EAR0087424 (M.N.D. and J.G.) from the Petrology and Geochemistry Program at NSF. Frank Spear generously provided the sample from the Valhalla complex. We are also grateful to him for a thoughtful critical review of the manuscript, which substantially improved the quality and clarity of the paper, especially with respect to the discussion of the results on the Valhalla sample.*[KF]*

References

[1] J. Ganguly, M. Tirone, Relationship between cooling rate and cooling age of a mineral; theory and applications to meteorites, Meteorit. Planet. Sci. 36 (2001) 167–175.
[2] F.S. Spear, R.R. Parrish, Petrology and cooling rates of the Valhalla Complex, British Columbia, J. Petrol. 37 (1996) 733–765.
[3] J. Ganguly, M. Tirone, R. Hervig, Diffusion kinetics of samarium and neodymium in garnet, and a method of determining cooling rates of rocks, Science 281 (1998) 805–807.
[4] R.G. Coleman, X. Wang, Ultrahigh Pressure Metamorphism, Cambridge University Press, 1995, 528 pp.
[5] U. Ring, M.T. Brandon, G.S. Lister, S.D. Willett, Exhumation Processes: Normal Faulting Ductile Flow and Erosion, Geol. Soc. London 154, 1999, 378 pp.
[6] S. Duchene, J.M. Lardeaux, F. Albarede, Exhumation of eclogites: insights from depth-time path analysis, Tectonophysics 280 (1997) 125–140.
[7] C.P. DeWolf, C.J. Zeissler, A.N. Halliday, K. Mezger, E.J. Essene, The role of inclusions in U-Pb and Sm-Nd garnet geochronology; stepwise dissolution experiments and trace uranium mapping by fission track analysis, Geochim. Cosmochim. Acta 60 (1996) 121–134.
[8] T.W. Argles, C.I. Prince, G.L. Foster, D. Vance, New garnets for old? Cautionary tales from young mountain belts, Earth Planet. Sci. Lett. 172 (1999) 301–309.
[9] M.H. Dodson, Closure temperature in cooling geochronological and petrological systems, Contrib. Mineral. Petrol. 40 (1973) 259–274.
[10] M.H. Dodson, Closure profile in cooling systems, in: P.F. Dennis, R. Freer (Eds.), Kinetics and Transport in Silicate and Oxide Systems, Materials Sciences Forum, Min. Soc. Great Britain, vol. 7, 1986, pp. 145–154.
[11] J. Ganguly, M. Tirone, Diffusion closure temperature and age of a mineral with arbitrary extent of diffusion; Theoretical formulation and applications, Earth Planet. Sci. Lett. 170 (1999) 131–140.
[12] D. Vance, R.K. O'Nions, Isotopic chronometry of zoned garnet; growth kinetics and metamorphic histories, Earth Planet. Sci. Lett. 97 (1990) 227–240.
[13] K.W. Burton, R.K. O'Nions, High-resolution garnet chronometry and the rates of metamorphic processes, Earth Planet. Sci. Lett. 107 (1991) 649–671.
[14] K. Mezger, E.J. Essene, A.N. Halliday, Closure temperature of the Sm-Nd system in metamorphic garnets, Earth Planet. Sci. Lett. 113 (1992) 397–409.
[15] S.R. Getty, J. Selverstone, B.P. Wernicke, S.B. Jacobsen, E. Aliberti, Sm-Nd dating of multiple garnet growth events in an arc-continent collision zone, northwestern U.S. Cordillera, Contrib. Mineral. Petrol. 115 (1993) 45–57.
[16] H.P. Liermann, J. Ganguly, Compositional properties of coexisting orthopyroxene and spinel in some Antarctic diogenites: Implications for thermal history, Meteorit. Planet. Sci. 36 (2001) 155–166.
[17] W.D. Carlson, C. Denison, Mechanisms of porphyroblast crystallization: results from high-resolution computed X-ray tomography, Science 257 (1992) 1236–1239.
[18] G.J. Wasserburg, S.B. Jacobsen, D.J. DePaolo, M.T. McCulloch, T. Wen, Precise determination of Sm/Nd ratios, Sm and Nd isotopic abundances in standard solutions, Geochim. Cosmochim. Acta 45 (1981) 2311–2323.
[19] M.N. Ducea, J.B. Saleeby, The age and origin of a thick mafic-ultramafic root from beneath the Sierra Nevada batholith, Contrib. Mineral. Petrol. 133 (1998) 169–185.
[20] M.N. Ducea, G. Sen, J. Eiler, J. Fimbres, Melt depletion and subsequent metasomatism in the shallow mantle beneath Koolau volcano, Oahu (Hawaii), Geochem. Geophys. Geosyst. (2002) 10.1029/2001GC000184.
[21] S.D. Carr, R.R. Parrish, R.L. Brown, Eocene structural development of the Valhalla Complex, British Columbia, Tectonics 6 (1987) 175–196.
[22] A.C. Lasaga, Geospeedometry, an extension of geothermometry, in: Saxena, S.K. (Ed.), Kinetics and Equilibrium in Mineral Reactions, Springer, New York, 1983, pp. 81–114.
[23] J. Ganguly, S. Dasgupta, W. Cheng, S. Neogi, Exhumation history of a section of Sikkim Himalayas, India: records in the metamorphic mineral equilibria and compositional zoning of garnet, Earth Planet. Sci. Lett. 183 (2000) 471–486.
[24] J.M. Ferry, F.S. Spear, Experimental calibration of the partitioning of Fe and Mg between biotite and garnet, Contrib. Mineral. Petrol. 66 (1978) 113–117.
[25] J. Ganguly, W. Cheng, S. Chakraborty, Cation diffusion in aluminosilicate garnets: experimental determination in

pyrope-almandine diffusion couples, Contrib. Mineral. Petrol. 131 (1998) 171–180.
[26] R.T. Hackler, B.J. Wood, Experimental determination of Fe and Mg exchange between garnet and olivine and estimation of Fe-Mg mixing properties in garnet, Am. Mineral. 74 (1989) 994–999.
[27] J. Crank, Mathematics of Diffusion, Oxford, 1975, 414 pp.
[28] J. Ganguly, H. Yang, S. Ghose, Thermal history of mesosiderites: Quantitative constraints from compositional zoning and Fe-Mg ordering in orthopyroxenes, Geochim. Cosmochim. Acta 58 (1994) 2711–2723.
[29] B.M. Page, The southern Coast Ranges, in: W.G. Ernst (Ed.), The Geotectonic Development of California; Rubey Vol. I, Prentice-Hall, Englewood Cliffs, NJ, 1981, pp. 329–417.
[30] C.A. Hall Jr., Geology of the Point Sur-Lopez Point region, Coast Ranges, California; a part of the Southern California Allochthon, Geological Society of America (GSA), Boulder, CO, 1991, 40 pp.
[31] R.R. Compton, Granitic and metamorphic rocks of the Salinian block, California Coast Ranges, in: Geology of Northern California, Bulletin – California, Division of Mines and Geology, California Division of Mines and Geology, San Francisco, CA, 1966, pp. 277–287.
[32] S. Kidder, M. Ducea, G. Gehrels, P.J. Patchett, J. Vervoort, Tectonic and magmatic development of the Salinian Coast Ridge Belt, California, Tectonics (2003) in press.
[33] K. Grove, Latest Cretaceous basin formation within the Salinian Terrane of west-central California, Geol. Soc. Am. Bull. 105 (1993) 447–463.
[34] C.W. Naeser, D.C. Ross, Fission-track ages of sphene and apatite of granitic rocks of the Salinian Block, Coast Ranges, California, J. Res. U.S. Geol. Surv. 4 (1976) 415–420.
[35] K.J. Ludwig, Isoplot/Ex (rev. 2.49), Berkeley Geochronology Center Spec. Publ. No. 1a, 2001, 56 pp.